Heating Rates and Enhanced Equilibration Rates with Strongly Correlated Ions in a Penning-Malmberg Trap[1]

J. J. Bollinger[*], M. J. Delaney[†], T. Hasegawa[**] and D. H. E. Dubin[‡]

[*]*National Institute of Standards and Technology, Boulder, CO 80305*
[†]*Dept. Phys., Univ. of Wisconsin, Madison, WI 53706*
[**]*Dept. Phys., Keio U, Kanagawa 223-8522, Japan*
[‡]*Dept. Phys., Univ. Calif. San Diego, La Jolla, CA 92093*

Abstract. We laser-cooled up to 10^6 $^9Be^+$ ions to $\sim$1 mK in a Penning-Malmberg trap and measured the ion temperature as a function of time after turning off the cooling laser. We observed a rapid heating of the ions when their temperature in a direction parallel to the magnetic field increased above 10 mK and show that this is due to the equilibration of a warm (few kelvins) impurity-ion cyclotron motion with the parallel motion of the $^9Be^+$ ions. The observed equilibration is more than 14 orders of magnitude faster than predicted by theory that is valid in the absence of correlations, and is closely related to the enhancement of nuclear reactions in dense stellar interiors, first predicted over 50 years ago by Salpeter. Future experiments similar to the work described here can be used to model nuclear fusion in dense plasmas. Finally, we describe an attempt to use the measured heating rate of the $^9Be^+$ ions to observe the latent heat of the predicted solid-liquid phase transition.

Keywords: cyclotron equilibration rate, laser cooling, latent heat, one-component plasma, Penning trap, strongly correlated plasma
PACS: 52.27.Gr, 52.27.Jt, 64.70.Dv, 32.80.Pj

INTRODUCTION

Strongly correlated (or strongly coupled) Coulomb systems encompass diverse many-body systems that exist over a wide range of densities and temperatures [1]. Examples include colloidal suspensions, complex (dusty) plasmas, laser-cooled trapped ions, and dense astrophysical matter. A particularly simple strongly coupled Coulomb system is the strongly coupled one-component plasma (OCP). An OCP consists of a single species of point charges embedded in a uniform, neutralizing background charge [2, 3]. The thermodynamic state of an OCP is determined by a single coupling parameter $\Gamma = q^2/(4\pi\varepsilon_0 a_{\rm WS} k_B T)$, where ε_0 is the vacuum permittivity, q is the ion charge, k_B is Boltzmann's constant, T is the temperature, and $a_{\rm WS}$ is the Wigner-Seitz radius, given by the expression for the plasma density $n_0 = 3/(4\pi a_{\rm WS}^3)$. Γ is a measure of the ratio of the potential energy between nearest-neighbor ions to the ion thermal energy. Extensive theoretical investigations have shown that a strongly coupled OCP ($\Gamma > 1$) undergoes a first-order solid-liquid phase transition at $\Gamma \simeq 172 - 174$ [2, 4]; however, there has been no experimental confirmation of this result. Strongly coupled OCPs

exist in dense astrophysical objects such as in the crust of a neutron star or in the interior of a white dwarf star, but can also exist at lower density if the temperature is correspondingly low. Laser-cooled trapped ions are a rigorous and convenient low-density, low-temperature realization of a strongly coupled OCP. In an ion trap the trapping fields are mathematically equivalent to a neutralizing background charge [5].

In this manuscript we describe measurements of the temperature of the $^9Be^+$ ion motion in a direction parallel to the applied magnetic field of the Penning trap as a function of time after turning off the cooling laser [6, 7]. With the cooling laser on we measure ion temperatures ~ 1 mK, close to the 0.5 mK Doppler laser cooling limit. With a typical ion density of $n_0 = 2 \times 10^8$ cm^{-3}, a 1 mK temperature gives a coupling of $\Gamma \sim 1500$, which is in the solid (i.e., crystalline) regime of the OCP phase diagram. Previous experiments have observed the predicted bcc crystals when the number of trapped ions was greater than $\sim 10^5$ [8, 9]. After the cooling laser is turned off, collisions with the room temperature residual gas produce a $\sim$0.1 K/s rise in the ion temperature until the ion temperature reaches 10 mK. With $n_0 = 2 \times 10^8$ cm^{-3}, 10 mK corresponds to $\Gamma \sim 170$, the predicted solid-liquid phase transition. For temperatures slightly greater than 10 mK, we observe an unexpected rapid heating of the $^9Be^+$ ions, which we show is due to the equilibration between the cold parallel motion of the $^9Be^+$ ions and the warm (few kelvins) cyclotron motion of heavier impurity ions that surround the $^9Be^+$ ions. In an uncorrelated plasma this equilibration is exponentially suppressed at the large magnetic fields and low temperatures of this experiment [10, 11]. The observed heating indicates that the equilibration of cyclotron motion with motion parallel to the magnetic field is enhanced in a strongly correlated plasma.

Theoretical work [12] has shown that the observed enhancement is closely related to the enhancement of nuclear reaction rates in dense stellar interiors where the correlation parameter Γ can be greater than 1. In a strongly correlated plasma the neighboring ions cannot be neglected when two ions undergo a close collision. The effect of the neighboring ions is to screen the Coulomb repulsion of the colliding ions, enhancing the probability of close collisions. In 1954 Salpeter showed that this enhancement of close collisions gives rise to an increase in nuclear fusion rates in the interior of dense stars [13, 14]. In particular Salpeter showed that when the nuclear fusion rate is predominantly due to binary collisions, then the fusion rate is enhanced by a factor $f(\Gamma)$ relative to the fusion rate calculated for an uncorrelated plasma with the same density and temperature. The factor $f(\Gamma)$ depends only on the Coulomb coupling parameter. The regimes $\Gamma < 1$ and $\Gamma > 1$ are called, respectively, the weak and strong screening regimes. In the strong screening regime $f(\Gamma) \sim e^{\Gamma}$, which produces huge enhancements even for moderate values of Γ. At very high densities binary collisions no longer dominate the nuclear fusion rate. In this regime, known as the pycnonuclear regime, the fusion rate is also enhanced, but the enhancement no longer simply depends only on the Coulomb coupling parameter. Dubin [12] has shown that weak and strong screening regimes can also be defined for the equilibration of ion cyclotron energy with ion energy parallel to the magnetic field in a Penning trap. In these weak and strong screening regimes the equilibration of ion cyclotron and parallel energies is enhanced by *exactly* the same factor predicted for nuclear fusion rates. Future experiments similar to those discussed here should be able to measure the Salpeter enhancement factor in the strong screening regime for the first time.

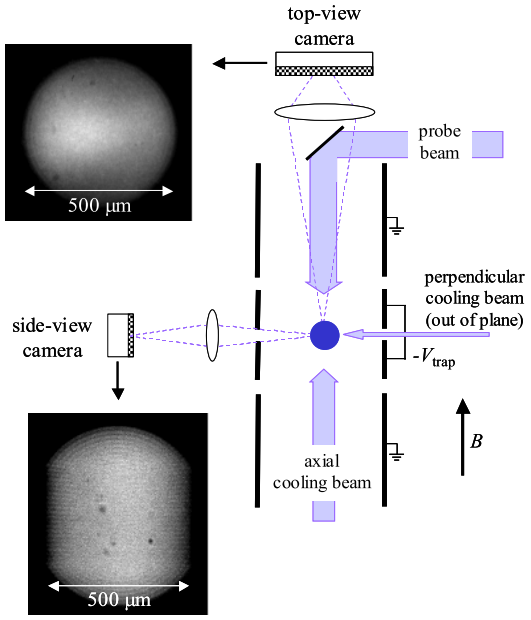

FIGURE 1. Schematic diagram of the setup. Figure is not to scale. The trap diameter is 4 cm. Top- and side-view images of a plasma with 26 000 ions are shown. The vertical edges of the plasma visible in the side-view image are due to the presence of non-fluorescing impurity ions heavier than $^9Be^+$.

HEATING RATE MEASUREMENTS

Figure 1 shows a schematic diagram of the setup [6]. The 4.5 T magnetic field of a superconducting solenoid with a room-temperature bore produces a $^9Be^+$ cyclotron frequency of $\Omega_c = 2\pi \times 7.6$ MHz. With a typical trapping voltage of $V_{\rm trap} = 500$ V, the $^9Be^+$ axial and magnetron frequencies are respectively $\omega_z = 2\pi \times 565$ kHz and $\omega_m = 2\pi \times 21$ kHz. The $E \times B$ fields cause the trapped ion plasma to rotate about the magnetic-field axis. The plasma evolves to a thermal equilibrium state where this rotation is rigid. At the low temperatures characterizing the present work, the plasma density is uniform. The rotation frequency ω_r determines the plasma density and the overall plasma shape [3]. We use a rotating electric field to precisely control ω_r [15]. The data presented here were taken on approximately spherical plasmas of 10^4 to 10^6 $^9Be^+$ ions with $\omega_r = 2\pi \times 64$ kHz, which corresponds to $n_0 = 2 \times 10^8$ cm^{-3} and $a_{\rm WS} \sim 10$ μm.

$^9Be^+$ ions are created in the trap by electron impact ionization of neutral ^9Be evaporated from an oven. By biasing the electron source so that the electrons have just enough energy to ionize ^9Be we create a pure $^9Be^+$ ion plasma. However, over many hours (time constant of several days) heavier singly charged ions [$m = 10$ (BeH^+), 26, 34 amu] are created by collisions between $^9Be^+$ and the room-temperature residual gas at $\sim 4 \times 10^{-9}$ Pa. The plasma rotation causes ions of different mass to centrifugally separate and the heavy-mass impurity ions occupy a region at larger radii (see Fig. 1).

The plasma is cooled by Doppler laser-cooling to $T \sim 1$ mK. Cooling laser beams are sent through the trap parallel and perpendicular to the magnetic field axis. The resulting resonance fluorescence is imaged by side- and top-view cameras. The cooling laser

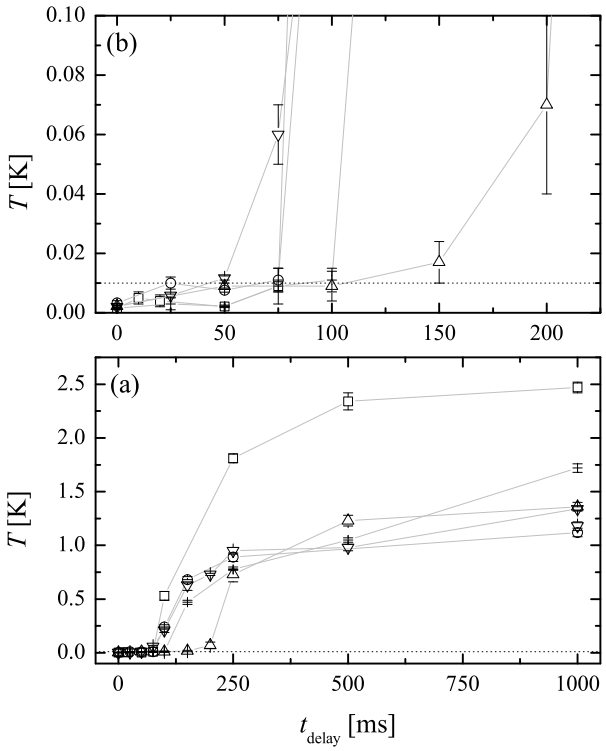

FIGURE 2. (a) Temperature curves recorded with different plasmas on different days spanning a period of many months. The horizontal dotted line indicates $T = 10$ mK. (b) is a close-up of (a).

is tuned approximately 20 MHz below the $^2S_{1/2}$ $(m_I = +\frac{3}{2}, m_J = +\frac{1}{2}) \leftrightarrow {}^2P_{3/2}$ $(m_I = +\frac{3}{2}, m_J = +\frac{3}{2})$ cycling transition. Over a $\sim$10 s time scale the cooling laser optically pumps 94% of the ions into the $^2S_{1/2}$ $(+\frac{3}{2}, +\frac{1}{2})$ state, i.e., the lower level of the cooling transition [16]. A probe beam is introduced along the magnetic field axis to measure the temperature associated with motion along this axis. The temperature is measured by Doppler laser spectroscopy on the single-photon transition $^2S_{1/2}$ $(m_I = +\frac{3}{2}, m_J = +\frac{1}{2}) \leftrightarrow {}^2P_{3/2}$ $(m_I = +\frac{3}{2}, m_J = -\frac{1}{2})$ [6, 16]. This transition depopulates the cooling cycle; that is it removes, in a Doppler sensitive way, some of the population from the $^2S_{1/2}$ $(+\frac{3}{2}, +\frac{1}{2})$ optically pumped ground state and puts it in the $^2S_{1/2}$ $(+\frac{3}{2}, -\frac{1}{2})$ ground-state hyperfine level. The change in the $^2S_{1/2}$ $(+\frac{3}{2}, +\frac{1}{2})$ state population is measured from the change in the cooling laser fluorescence. After each probe laser measurement, the cooling laser beams are applied for about 20 s to re-initialize the optically pumped state. See Refs. [6, 16] for details.

We measured the temperature as a function of the time t_{delay} after turning off the cooling laser beams. Figure 2 shows temperature curves obtained with different plasmas, all with the same density $n_0 = 2 \times 10^8$ cm^{-3}, over a period of many months. In all cases, the temperature increased slowly (~ 0.1 K/s) until $T \simeq 10$ mK ($\Gamma \sim 170$), which is the temperature associated with the solid-liquid phase transition. At 10 mK, a sudden increase to temperatures of a few kelvins takes place. The onset of this rapid heating

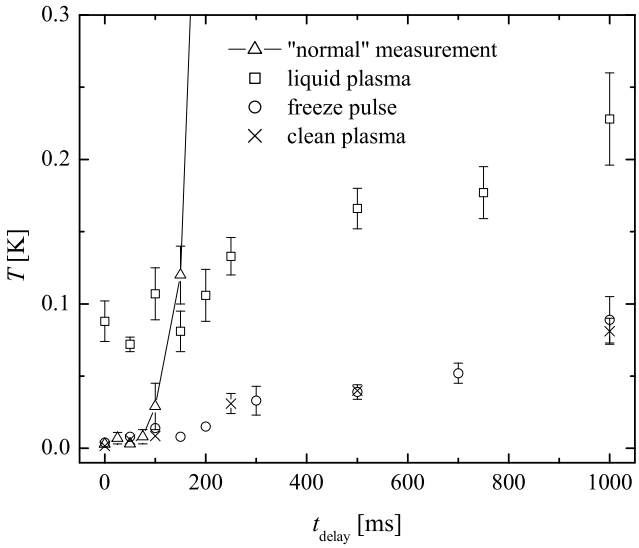

FIGURE 3. Temperature curves recorded using different initial conditions. The “normal" curve (△) was obtained using both parallel and perpendicular laser-cooling. Only perpendicular laser-cooling was applied in case of the “liquid" curve (squares). The freeze-pulse method (discussed in the last section on the heating rate and the latent heat) was used to obtain the curve indicated with circles. These three curves were recorded on 56 000 ion plasmas with ~ 35 % impurity ions. The curve shown with $\times$ was recorded on a 23 000 ion plasma containing no impurity ions.

occurs at different values of t_{delay}, depending on the magnitude of the slow heating rate in the solid phase, but always occurs at approximately the same temperature $T \simeq 10$ mK. A measurement of the temperature of the $^9Be^+$ motion perpendicular to the magnetic field axis showed similar behavior.

We varied a number of experimental parameters and conditions to investigate their effect on the heating curve. From temperature curves recorded with different residual gas pressures we determined in Ref. [6] that the slow ~ 0.1 K/s heating rate measured in the solid phase is due to collisions between trapped ions and room-temperature residual gas molecules. Increasing the residual gas pressure also increased the size of the rapid heating step that occurred when the parallel temperature of the $^9Be^+$ ions increases above 10 mK. In addition to the residual gas pressure, the only other experimental condition that had a significant effect on the heating curve was the presence (or absence) of impurity ions. Figure 3 shows a temperature curve (the $\times$’s) taken on a “clean” plasma containing essentially no impurity ions. A $^9Be^+$ plasma free of impurity ions is obtained for a few hours after creating the plasma. There is no rapid heating step in this curve; rather the $^9Be^+$ temperature smoothly increases at the slow ~ 0.1 K/s rate for the duration for the 1 s measurement.

These dependencies of the rapid heating step on residual gas pressure and impurity ions indicate that the heating step is likely due to an equilibration of the $^9Be^+$ ion parallel motion with an impurity-ion motion that is excited by residual gas collisions. Theory and molecular dynamics simulations [7] show that laser-cooled $^9Be^+$ ions efficiently cool the parallel motion of the impurity ions, but in the crystalline regime, not the impurity ion cyclotron motion. Estimates of the sympathetic cooling rate for the impurity

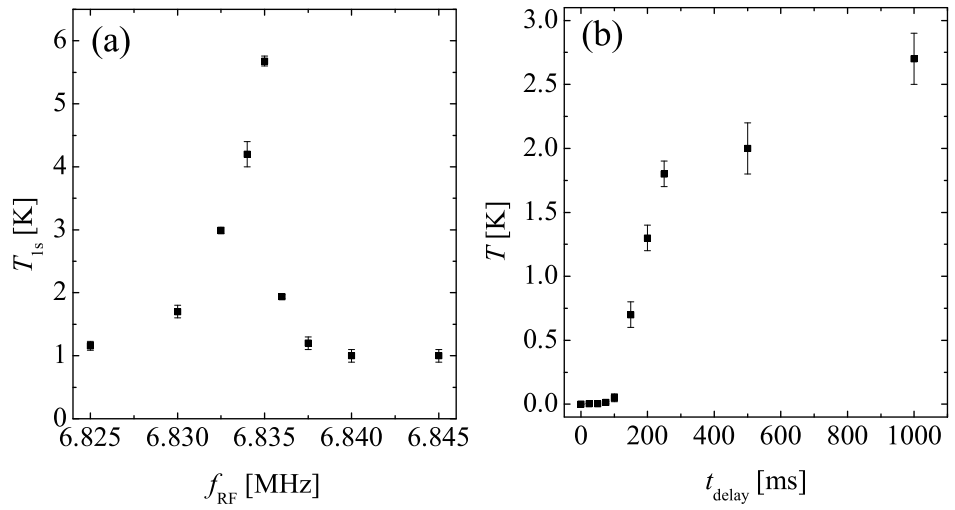

FIGURE 4. (a) The temperature at $t_{\rm delay} = 1$ s as a function of the frequency of an rf field exciting the mass-10 cyclotron motion. (b) A temperature curve recorded with the rf drive tuned near resonance. Figs. (a) and (b) were recorded on different plasmas. In (b) the temperature at $t_{delay} = 1$ s without the rf drive was ~ 0.7 K.

ion cyclotron motion along with the measured residual gas heating rate (~ 0.1 K/s) indicate likely impurity ion cyclotron temperatures of $\sim$1 K, which is the correct order of magnitude to account for the observed heating step.

By exciting the mass-10 cyclotron motion with an rf field, we showed experimentally [7] that additional excitation of the impurity-ion cyclotron motion increases the amount of rapid heating. Figure 4 shows the $^9Be^+$ temperature at $t_{\rm delay} = 1$ s as a function of the rf frequency, and a full temperature curve recorded with the rf drive tuned near the mass-10 resonance. A strong dependence of the heating step on the rf drive frequency (and therefore the mass-10 impurity ion energy) is observed. In addition the energy added to the impurity-ion cyclotron motion is not coupled with the $^9Be^+$ parallel motion until $T_{\|,{\rm Be}^+} \sim 10$ mK. These measurements, along with the theory and molecular dynamics simulations of the sympathetic cooling rates, indicate that the source of the energy released in the rapid heating step is a warm (few kelvins) cyclotron motion of the trapped impurity ions.

COMPARISON WITH THEORY

The rapid heating step is an example of an equilibration of an ion cyclotron energy with the energy of ion motion parallel to the magnetic field. When $T_{\|,{\rm Be}^+}$ increases above 10 mK the temperature measurements in Fig. 2 indicate that the equilibration occurs in less than 1 s (i.e. an equilibration rate $\nu \geq 1$ s^{-1}). It is interesting to compare this observed rate with theory. Until recently, the only theoretical treatment [10] of the equilibration of ion cyclotron and parallel energies in a Penning trap was valid only for $\Gamma \ll 1$. In this theory, which is well tested experimentally [11], cyclotron energy is shared with parallel energy through close collisions where the distance of closest approach b in the

collision is comparable to the ion cyclotron radius r_c. For large magnetic fields and low temperatures the mean distance of closest approach can be much larger than the mean cyclotron radius ($\langle b \rangle \gg \langle r_c \rangle$). In this case the plasma is called strongly magnetized, and close collisions that share cyclotron energy with parallel energy are rare. This results in an equilibration rate that is exponentially small in the ratio $\kappa \equiv (\langle b \rangle / \langle r_c \rangle)/\sqrt{2}$ [10]. With experimental parameters appropriate for the experiments discussed here ($^9Be^+$, $B = 4.5$ T, $T_\parallel \sim 50$ mK, $n_0 = 2 \times 10^8$ cm^{-3}), the theory of Ref. [10] (valid for $\Gamma \ll 1$) predicts an equilibration rate $\nu_0 \sim 10^{-15}$ s^{-1}. This geologically slow rate is more than 14 orders of magnitude slower than the observed equilibration rate.

However, as briefly discussed in the introduction, close collisions can be enhanced in a correlated plasma due to screening from the neighboring ions. Weak and strong screening regimes can be identified in a strongly magnetized plasma where the cyclotron/parallel equilibration rate is enhanced by the same factor $f(\Gamma)$ predicted for the nuclear fusion rate in dense stellar interiors [13, 14]. With the experimental parameters used to calculate ν_0 in the previous paragraph, $\Gamma \sim 30$ and the Salpeter screening factor is $e^\Gamma \sim 10^{13.6}$, which, within an order of magnitude, is the enhancement required to explain the observed equilibration. However, the agreement is fortuitous, as the measurements of Fig. 2 are from plasmas in the high density pycnonuclear regime where binary collisions no longer dominate the equilibration rate. Presently no detailed theory exists for cyclotron/parallel equilibration in the pycnonuclear regime. Nevertheless our measurements indicate that this equilibration rate is strongly enhanced in a plasma with $\Gamma \gg 1$.

In Ref. [12] Dubin shows that the weak and strong screening regimes where the cyclotron/parallel equilibration is predominantly due to binary collisions occurs when $\Gamma < \kappa^{2/5}$. (The strong magnetization parameter κ is defined in Ref. [10] and in the first paragraph of this section.) This regime can be accessed by carrying out measurements at lower densities and higher temperatures than reported here. Instead of measuring the coupling of an elevated (and not measured) impurity-ion cyclotron temperature with the $^9Be^+$ parallel temperature we could directly measure the equilibration between the $^9Be^+$ parallel and cyclotron motions by using an rf drive to heat the $^9Be^+$ cyclotron motion. The $^9Be^+$ cyclotron temperature could also be measured as a function of time after turning off the cooling laser. In this way it should be possible to measure the Salpeter screening factor for the first time in the strong screening ($\Gamma > 1$) regime. Experiments like this can advance our understanding of nuclear reactions in dense stellar plasmas.

HEATING RATE AND THE LATENT HEAT

In addition to the clean plasma (i.e., no impurity ions) temperature measurements, Fig. 3 shows several different temperature curves recorded with different initial conditions. The measurements indicated by the squares were obtained with perpendicular laser cooling only, that is, the cooling laser beam that is normally directed along the magnetic field axis was blocked. With the perpendicular cooling laser on, we measured $T_{\parallel,Be^+} \sim$ 70 mK, which corresponds to a liquid plasma. This warmer parallel temperature is expected because the parallel motion is only indirectly cooled through its coupling to

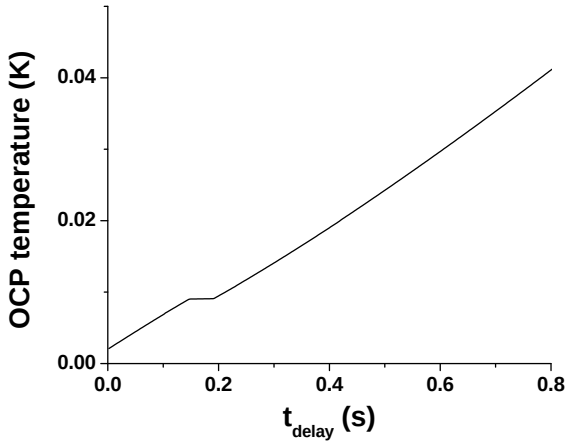

FIGURE 5. Calculation of the heating rate of an OCP assuming a density of 2×10^8 cm^{-3} and a constant 0.1 K/s heating rate. The $\sim$50 ms pause in the temperature increase at $\sim$10 mK is due to the latent heat of the solid-liquid phase transition.

the perpendicular motion, but is directly heated by photon recoil. Starting with a liquid plasma, a rapid heating step is not observed. Instead $T_{\|,\mathrm{Be}^+}$ smoothly increases at the slow $\sim$ 0.1 K/s heating rate due to residual gas collisions.

From our understanding of the rapid heating step developed in the previous section, this behavior is in fact expected. In the liquid state at $T_{\|,\mathrm{Be}^+} \sim 70$ mK the coupling between the impurity ion cyclotron motion and the $^9\mathrm{Be}^+$ motion is significantly greater than in the crystalline state. This strong coupling prevents residual gas collisions from elevating the impurity-ion cyclotron temperature. Starting with a liquid plasma we can also prepare a crystalline plasma with a low impurity-ion cyclotron temperature by freezing the plasma with a short parallel laser cooling pulse. This is to be contrasted with the "normal" temperature measurements where the parallel laser beam is applied for the $\sim$20 s optical pumping period between temperature measurements. The freeze-pulse data in Fig. 3 show temperature measurements obtained with a 100 ms parallel laser-cooling pulse applied immediately before turning off the cooling lasers. In this case the plasma is a solid at the start of the heating measurement, but spends less than 100 ms in the solid phase, where the sympathetic cooling rate is weak. No additional heating is observed at the solid-liquid phase transition.

By working with plasmas with small numbers of impurity ions and by using the freeze-pulse technique, we can get rid of the rapid heating step and obtain a constant $\sim$ 0.1 K/s heating rate due to residual gas collisions in both the crystalline and liquid regimes. Figure 5 shows a calculation of the expected temperature increase for a $^9\mathrm{Be}^+$ ion plasma, assuming a constant 0.1 K/s heating rate. The calculation assumes (1) that the plasma energy can be written as the sum of the zero-temperature mean-field electrostatic energy E^0 of the plasma plus the internal energy U of a bulk OCP (valid for large plasmas [3]), and (2) E^0 is constant as the plasma temperature increases. The $\sim$50 ms pause in the temperature near 10 mK is due to the latent heat of first-order solid-liquid phase transition. At the phase transition, the ion temperature stays constant until the plasma absorbs the latent heat required to melt the crystal. Is it possible to observe

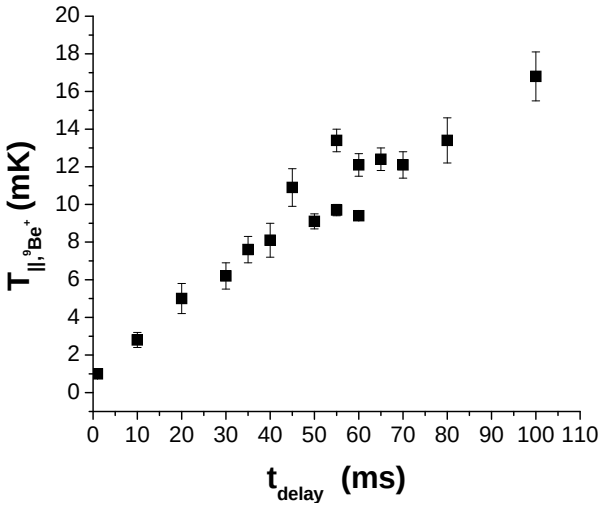

FIGURE 6. Carefully measured temperature curve on an approximately spherical plasma of 4×10^5 $^9Be^+$ ions obtained with the freeze-pulse technique. The measurements are not sufficiently accurate and stable to observe the predicted latent heat

this manifestation of the latent heat [3, 17] in the heating rate measurements?

Figure 6 shows our best attempt at observing the latent heat with this technique. The measurements were performed with the freeze-pulse technique within 36 hours of loading a plasma of 4×10^5 $^9Be^+$ ions. The probe laser frequency was controlled by varying the off-set frequency of a lock to a saturated absorption feature in an I_2 cell. Although Fig. 6 gives a hint of a pause in the $^9Be^+$ heating rate near the expected solid-liquid phase transition, the temperature measurements are not sufficiently accurate and stable to definitively observe (or not observe) the predicted latent heat. One problem is that the temperature measurements are slow. Each point in Fig. 6 corresponds to more than 1 hour of data taking. This could be improved by an order of magnitude by using a third laser to repump those ions tagged by the probe laser.

Although the measurements of Fig. 6 do not identify a latent heat, they do place some impressive limits on the stability of the plasma. In a trapped ion plasma the zero-temperature mean-field electrostatic energy E^0 is much larger than the internal energy U. Therefore a small change in E^0 can release a large amount of thermal energy. For example, we know the rotating wall provides phase-locked control of ω_r in the solid regime. However, because a liquid plasma does not sustain the shearing force of a solid plasma, could there be a very small slip in ω_r as the plasma undergoes the solid-liquid phase transition? For the plasma in Fig. 6, a 10 Hz decrease in the 64 kHz rotation frequency would increase the radius of the plasma by $\sim 0.1\ \mu$m ($\delta R_p/R_p \sim 1.3 \times 10^{-4}$). This slight radial expansion of the plasma would result in a decrease in the mean-field electrostatic energy of the plasma and a resultant $\sim$ 500 mK/ion release of thermal energy. The consistency of the temperature measurements of Fig. 6 means that the plasma radius and density are very constant while residual gas collisions heat the plasma. Observation of the latent heat through the plasma heating rate may be possible, but requires an extremely stable plasma and plasma heating rate for the duration of the

measurement. An experimental observation of the phase transition might be more easily done through Bragg scattering [8].

ACKNOWLEDGMENTS

We thank Dr. N. Shiga and Dr. R. J. Epstein for their comments on the manuscript. Construction of the apparatus and the initial experimental measurements described here were supported by the US Office of Naval Research.

REFERENCES

1. V. E. Fortov, K. I. Golden, and G. E. Norman, editors, *Proceedings of the International Conference on Strongly Coupled Coulomb Systems, Moscow, 2005*, J. Phys. A **39**, 4309, 2006.
2. S. Ichimaru, H. Iyetomi, and S. Tanaka, *Phys. Rep.* **149**, 91–205 (1987).
3. D. H. E. Dubin, and T. M. O'Neil, *Rev. Mod. Phys.* **71**, 87–172 (1999).
4. D. H. E. Dubin, *Phys. Rev. A* **42**, 4972 (1990).
5. J. H. Malmberg, and T. M. O'Neil, *Phys. Rev. Lett.* **39**, 1333–1336 (1977).
6. M. J. Jensen, T. Hasegawa, and J. J. Bollinger, *Phys. Rev. A* **70**, 033401 (2004).
7. M. J. Jensen, T. Hasegawa, J. J. Bollinger, and D. H. E. Dubin, *Phys. Rev. Lett.* **94**, 025001 (2005).
8. J. N. Tan, J. J. Bollinger, B. Jelenković, and D. J. Wineland, *Phys. Rev. Lett.* **75**, 4198–4201 (1995).
9. W. M. Itano, J. J. Bollinger, J. N. Tan, B. Jelenković, X.-P. Huang, and D. J. Wineland, *Science* **279**, 686–689 (1998).
10. M. E. Glinsky, T. M. O'Neil, M. N. Rosenbluth, K. Tsuruta, and S. Ichimaru, *Phys. Fluids B* **4**, 1156–1166 (1992).
11. B. R. Beck, J. Fajans, and J. H. Malmberg, *Phys. Rev. Lett.* **68** (1992).
12. D. H. E. Dubin, *Phys. Rev. Lett.* **94**, 025002 (2005).
13. E. E. Salpeter, *Australian J. Phys.* **7**, 353 (1954).
14. E. E. Salpeter, and H. M. van Horn, *Astrophys. J.* **155**, 183 (1969).
15. X.-P. Huang, J. J. Bollinger, T. B. Mitchell, and W. M. Itano, *Phys. Rev. Lett.* **80**, 73–76 (1998).
16. L. R. Brewer, J. D. Prestage, J. J. Bollinger, W. M. Itano, D. J. Larson, and D. J. Wineland, *Phys. Rev. A* **38**, 859–873 (1988).
17. J. P. Schiffer, *Phys. Rev. Lett.* **88**, 205003 (2002).